8

Parameterisation of the Four Half-Day Daylight Situations

Stanislav Darula and Richard Kittler
Institute of Construction and Architecture, Slovak Academy of Sciences, Bratislava, Slovakia

1. Introduction

The International Commission on Illumination (C.I.E) in its Technical Committee TC 3-08 for Daylight initiated in 1983 the so called International Daylight Measurement Programme (IDMP). This programme was officially launched by the CIE President Bodmann (1991) and several CIE IDMP stations were established world-wide and now relatively long-term regular data are available for studies and analysis (Kittler et al., 1992). Although some daily courses served to characterise luminance sky patterns and local daylight climate, there are possible more detail analysis of half-day situations with relation to sunshine duration, cloudiness and turbidity influences parametrised. This chapter tries to show the theoretical basis with documented applications using examples of several parametrised evaluations of measurements taken at the Bratislava and Athens CIE IDMP general stations which can be taken as instructing samples to be imitated using local measured data. The aim is also to show how momentary illuminance values correspond with hourly averages under four different daylight situations and how these half-day situations can be simulated when only monthly relative sunshine duration is available and when monthly or year-round random daylight conditions are needed and could be approximated.

2. Regular daylight measurements and their possible analysis

Since the CIE (2003) and ISO (2004) fifteen general homogeneous sky luminance patterns were standardised many CIE IDMP (International Daylight Measurement) stations recording regularly long-term daylight parameters try to evaluate the frequency of typical skies in their localities. Because the general CIE IDMP stations without sky luminance scanners sometimes do not record even zenith luminance L_{vz} simultaneously with diffuse skylight illuminance measurements D_v there are missing either sky scans or the classifying parameter L_{vz} / D_v, which could identify the momentary sky type. Thus, usually are only available data of regularly measured illuminance parameters in one minute steps during daytime, i.e.:

- Global horizontal illuminance by an unshaded detector G_v,
- Diffuse skylight illuminance on a horizontal sun-shaded detector D_v,
- Parallel sunbeam illuminance is sometimes measured by a sun tracker with a sky-shading cylinder and a detector placed perpendicularly to sunbeam flux $P_{v\perp}$,
- Global vertical illuminances on planes oriented to North G_{vvN}, East G_{vvE}, South G_{vvS} and West G_{vvW} excluding the ground reflection.

A clock controling system starting every minute count has to be recorded too either in local clock time LCT or true solar time TST. These regular measurements can serve for the specification of daylight situations during the half-day or to the rough identification of the sky type in any minute, hour or date.

In fact even in absence of the sun tracker the $P_{v\perp}$ illuminance can be derived from G_v and D_v recordings as

$$P_{v\perp} = \frac{G_v - D_v}{\sin\gamma_s} = \frac{P_v}{\sin\gamma_s} \ \text{[lx]}, \quad (1)$$

where $P_v = P_{v\perp}\sin\gamma_s$ is the horizontal illuminance caused by only parallel sunbeams in lx, γ_s is the momentary solar altitude which can be determined for any station location, date and clock time after:

$$\sin\gamma_s = \sin\varphi\sin\delta - \cos\varphi\cos\delta\cos(15°H) \ [-]. \quad (2)$$

The station location is given by the geographical latitude φ in deg., while date is specified by solar declination δ and hour number H during daytime in TST.

Solar declination angle can be calculated for any day number within a year J (i.e. for 1st January $J = 1$ and for 31st December $J = 365$) using different approximate equations (e.g. Kittler & Mikler, 1986). The simplest is that introduced by Cooper (1969)

$$\delta = 23.45°\sin\left[\frac{360°}{365}(284 + J)\right] \ [°], \quad (3)$$

and a more accurate approximation was recommended by EU after Gruter (1981)

$$\delta = 23.45°\sin\left[\frac{360°}{365}(J - 80.2°) + 1.92°\sin(J - 280°)\right] \ [°]. \quad (4)$$

Because usually CIE IDMP stations record all measurements in local clock time LCT the value H in TST has to be recalculated without consideration of summer shift time, after

$$H = LCT + \eta + \frac{(\lambda_z - \lambda_L)}{15°} \ \text{[h]}, \quad (5)$$

where η is the equation of time in hours approximated after a simpler formula by Pierpoint (1982)

$$\eta = 0.17\sin\left[4\pi(J - 80)/373\right] - 0.129\sin\left[2\pi(J - 8)/355\right] \ \text{[h]}, \quad (6)$$

or a more accurate formula by Heindl & Koch (1976)

$$\begin{aligned}\eta = {} & 0.008\cos\frac{360°J}{365} - 0.052\cos 2\frac{360°J}{365} - 0.001\cos 3\frac{360°J}{365} - \\ & -0.122\sin\frac{360°J}{365} - 0.157\sin 2\frac{360°J}{365} - 0.005\sin 3\frac{360°J}{365}\end{aligned} \ \text{[h]}, \quad (7)$$

λ_z is geographical longitude of the time zone in deg.,
λ_L - geographical longitude of the location in deg.
The perpendicular parallel sunbeam illuminance at the ground level can be also calculated applying the Bouguer law, i.e.

$$P_{v\perp} = LSC \in \exp\left(-a_v \, m T_v\right) \text{ [lx]}, \tag{8}$$

where LSC is the luminous solar constant (Darula et al., 2005), which is the normal extraterrestrial illuminance on the outer border of the atmosphere for the average distance between sun and earth, approximately $LSC = 133800$ lx., which is corrected for any date by the ellipticity factor $\in$, which is often approximated by IESNA (1984)

$$\in = 1 + 0.034 \cos \frac{360°}{365}\left(J - 2 \right) \text{ [-]}, \tag{9}$$

m - relative optical air mass approximated by Kasten & Young (1989)

$$m = \frac{1}{\sin \gamma_s + 0.50572\left(\gamma_s + 6.07995° \right)^{-1.6364}} \text{ [-]}, \tag{10}$$

a_v - luminous extinction coefficient of a clean and dry (Rayleigh) atmosphere after Clear (1982), later published by Navvab et al., (1984)

$$a_v = \frac{0.1}{1 + 0.0045 m} \text{ [-]}, \tag{11}$$

or

$$a_v = \frac{1}{9.9 + 0.043 m} \text{ [-]}, \tag{12}$$

T_v - luminous turbidity factor, which defines the number of clean and dry atmospheres in the direction of sunbeams that reduces relatively its momentary penetration. In fact, if in eq. (8) $P_{v\perp}$ is measured by a sun tracker or P_v is derived from measured $G_v - D_v$ data, then the actual value T_v can be determined as

$$T_v = \frac{-\ln\left(P_{v\perp} / \left(\in LSC\right)\right)}{a_v \, m} = \frac{\ln\left(E_v / P_v\right)}{a_v \, m} \text{ [-]}, \tag{13}$$

where $P_v = G_v - D_v$ and the extraterrestrial horizontal illuminance E_v is

$$E_v = \in LSC \sin \gamma_s \text{ [lx]}. \tag{14}$$

Thus, once the momentary illuminance $P_{v\perp}$ or P_v is determined the actual sunlight impact on any arbitrary plane can be calculated using the cosine of its incidence angle. However, for the vertical planes oriented either to direct East or West cardinal points this cosine function is simplified to

$$P_{vvE} = P_{vvW} = P_{v\perp} \cos\delta \sin\left(15°\left|12 - H\right|\right) \text{ [lx]}. \quad (15)$$

Note, that the East and West oriented vertical planes or fasades are exposed to the morning and afternoon half-day sunlight and skylight effects as measured by global vertical illuminances G_{vvE} or G_{vvW} respectively. So, when the direct sunlight using eq. (15) can be subtracted only diffuse skylight components for these orientations can be determined, i.e. D_{vvE} or D_{vvW} .

3. Four typical half-day situations indicated by illuminance courses

In the previous paper (Darula & Kittler, 2004a) from typical half-day illuminance courses were identified four characteristic daylight situations, which need to be explained in more detail:

Situation 1: Absolutely cloudless half-day with relative sunshine duration $s \geq 0.75$ and the parameter of instability $U \leq 8.4$ is almost clear with only few smaller clouds moving over the sky vault. Except these few sunshaded events the clear sky is quite stable and all horizontal illuminance parameters P_v , G_v and D_v follow a fluent increase in level during the morning hours and similar decrease during the afternoon due to solar altitude changes in different seasons.

Examples of selected half-days with *situation 1* are using recorded data from the Bratislava CIE IDMP general station (φ = 48°10´N, λ_L = 17°05´E) with the Central European climatic influences, but these should be taken as instructional and illustrative examples characterising typical cases of *situation 1.* As examples of clear sky mornings in Bratislava, Slovakia, were chosen courses measured during a long summer day on the 20th July 2006 followed by an autumn day on 22nd September 2007, while a short winter day 26th December 2006 represents one of the shortest days and the spring day 8th April 2006 with slight veiling Cirro-Stratus influences is also documented. The measured half-day courses of global horizontal illuminance G_v and diffuse sky illuminance D_v are documented in Fig. 1. Although the measurement registration is in the local clock time without the summertime shift it is evident that the courses follow the solar altitude changes, i.e. the $\sin\gamma_s$ tendency of the extraterrestrial horizontal illuminance after eq. (14). Therefore the efficiency parameters G_v / E_v and P_v / E_v should be rather stable and showing a large amount of the extraterrestrially available luminous flux reaching the ground level, therefore these parameters can markedly characterise *situation 1* (Fig. 2). The momentary 1-minute measurements except some slight spreads on the April day show a steady rise with the solar altitude which is even better followed by the hourly averages in Fig. 3 with the stepwise rise of G_v / E_v from 0.45 to 0.75. In consequence, also the luminous turbidity factors T_v follow the stable atmospheric conditions without abrupt changes, except when the sun position is shaded by crossing cloud patches and then can reach higher short time peaks as in Fig. 4 on 8th April 2006. However, due to gradual evaporation during morning the turbidity might fluently rise with the formation of Cirrus or Cirrostartus veiling cloudiness as is shown by the trend of rising hourly average T_v values in a small range 1.5 to 3 in Fig. 5. Such rising T_v effects can be expected especially in equatorial regions with sometimes gradual cloud formation at noontime and in afternoon hours, which no longer belong to *situation 1.*

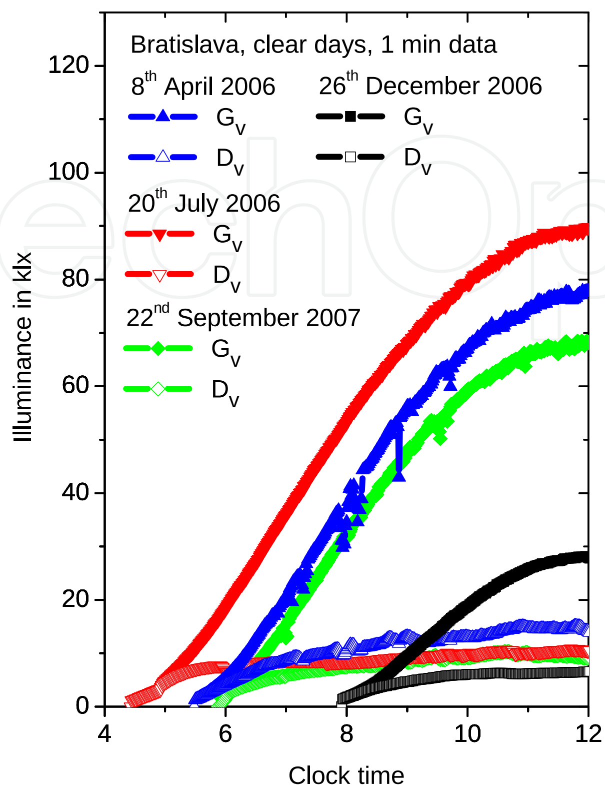

Fig. 1. Illuminance courses during clear morning *situations 1*

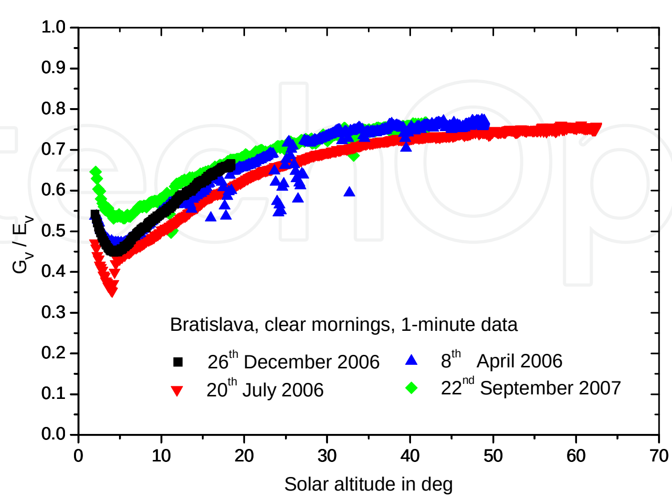

Fig. 2. G_v / E_v courses under *situation 1* after 1-minute measurements

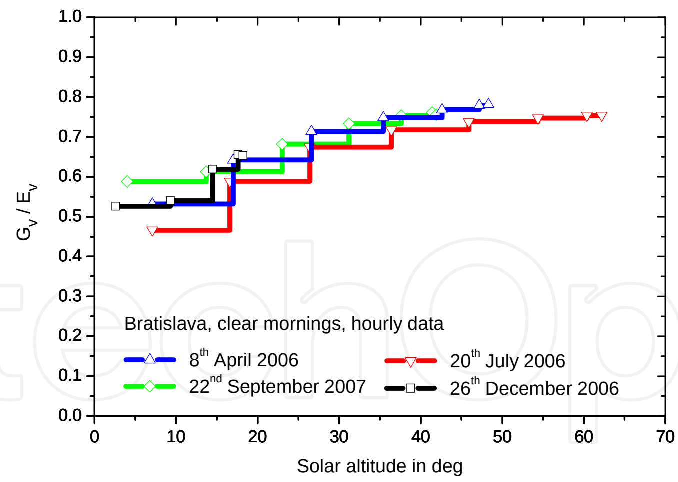

Fig. 3. G_v / E_v courses under *situation 1*:after measured hourly averages

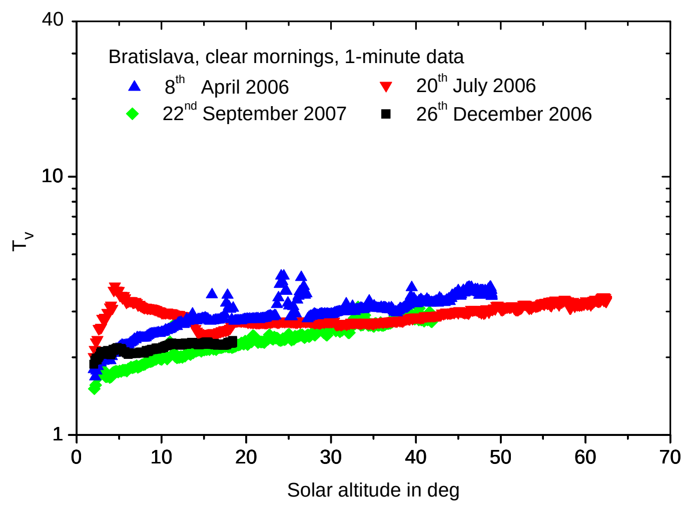

Fig. 4. T_v courses under *situation 1*: after 1-minute measurements

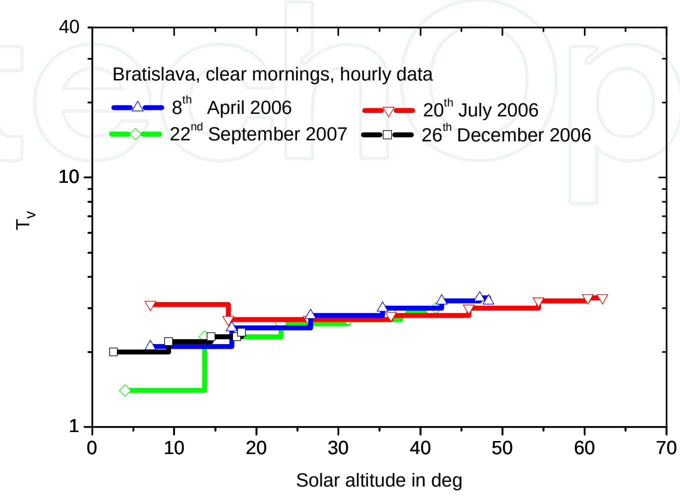

Fig. 5. T_v courses under *situation 1*: after measured hourly averages

It has to be noted that during sunrise and early morning hours the prevailing daylight is caused by skylight and therefore also on clear days the early G_v / E_v values are equal or quite close to D_v / E_v while under higher solar altitude the P_v / E_v component is rising while D_v / E_v value fluently decreases after Fig. 6 from roughly 0.5 to 0.1. The average hourly decrease is slightly distorting this range showing approximately 0.4 to 0.1 respectively (Fig. 7).

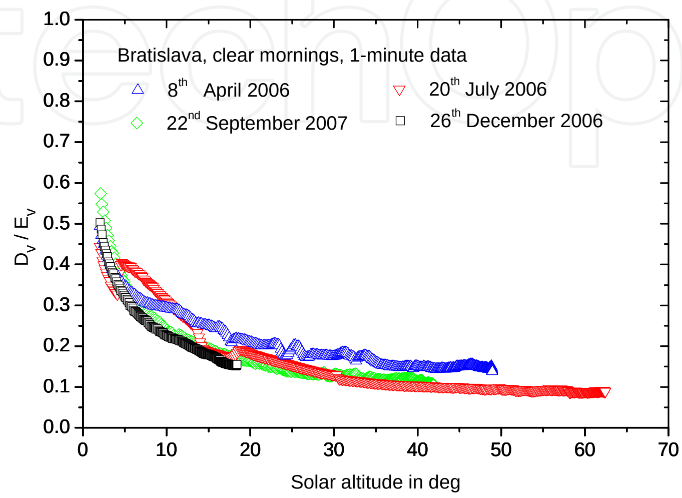

Fig. 6. D_v / E_v courses under *situation 1*: after 1-minute measurements

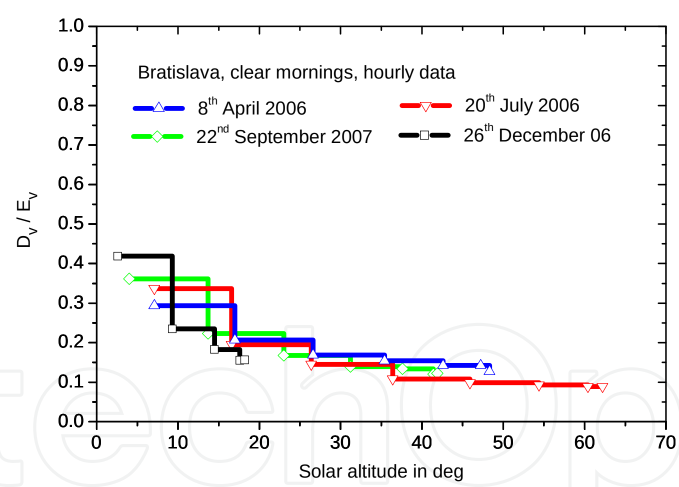

Fig. 7. D_v / E_v courses under *situation 1*: after measured hourly averages

If simultaneous measurements of the zenith luminance is recorded under clear sky conditions the classifying parameters L_{vz} / D_v, can identify the momentary sky type with the fluent rising tendency dependent on the solar altitude. In Fig. 8 this tendency is shown using 1-minute data while in Fig. 9 the same is documented after hourly mean values. Due to rather constant and fluent trends during *situation 1* besides the momentary one-minute recordings also hourly averages and appropriate parameters are quite satisfactorily reflecting clear half-days which might reduce the number of data considerably (Darula. & Kittler, 2005a).

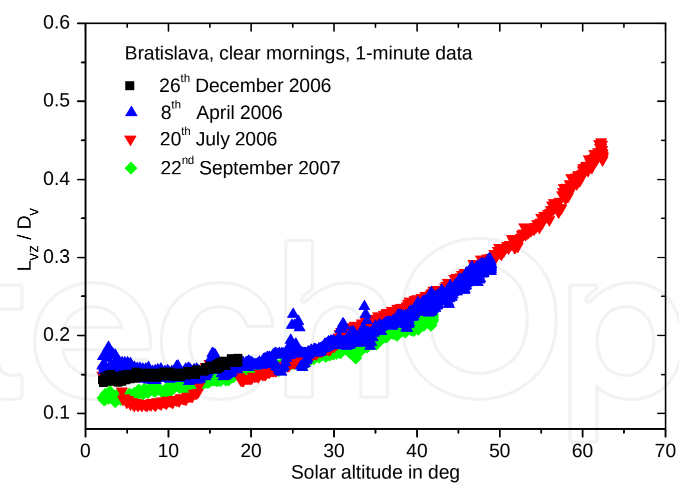

Fig. 8. L_{vz} / D_v courses under *situation 1*: after 1-minute measurements

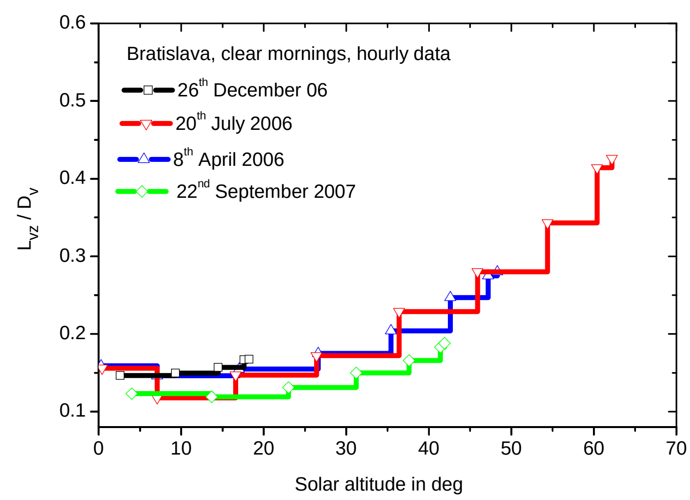

Fig. 9. L_{vz} / D_v courses under *situation 1*: after measured hourly averages

It is evident that the time period close to sunrise is untrustworthy due to an interval when solar altitude is zero and average G_v / E_v ratios are also reduced due to close to horizon mist or high turbidities. The minute courses are intersected by the hourly level in the point of hourly average solar altitude after Kittler & Mikler (1986)
where H_1, H_2 are consecutive hours

$$\gamma_{sH} = \frac{180°}{\pi} \arcsin\left[\sin\varphi \sin\delta + \frac{12}{\pi}\left(\sin\frac{\pi H_1}{12} - \sin\frac{\pi H_2}{12} \right) \right] \cos\varphi \cos\delta \ \text{[rad]}, \tag{16}$$

Sunrise hour H_{sr} when $\gamma_s = 0°$ is for any location and date defined by

$$H_{sr} = \frac{1}{15°} \arccos\left(\tan\varphi \tan\delta \right) \ \text{[h]}, \tag{17}$$

and due to symmetry around noon the hour of sunset H_{ss} = 24 - H_{sr} and the astronomically possible sunshine duration S_{ahd} during a half-day is

$$S_{ahd} = \frac{1}{15°} \arccos\left(-\tan\varphi \tan\delta\right) \text{ [h]}. \tag{18}$$

This is an normalising amount to calculate relative sunshine duration during the half-day s_{hd} if the true measured sunshine duration in hours S_{hd} is available:

$$s_{hd} = \frac{S_{hd}}{S_{ahd}} \text{ [-]}. \tag{19}$$

In the half-day system relative sunshine duration during the morning half-day is $s_{hd} = s_m$ while its afternoon relative duration is $s_{hd} = s_a$ either in absolute values or % respectively.
If regular minute recordings are measured, then S_{hd} can be calculated as the sum of all data after the WMO (1983) and CIE 108 (1994) when the direct irradiance $P_{e\perp} \geq 120$ W/m² taken in hours or their decimals.

Situation 2: Cloudy half-days with possible foggy short periods are characterised by scarce and lower sunlight influences under a range of relative sunshine durations ($0.03 \leq s \leq 0.75$ and $U \leq 10 - 6s$) and relatively higher diffuse illuminance levels. Such situations are caused by the prevailing area of the sky covered from almost homogeneous presence of clouds layers with different combinations of cloud type, turbidity and cloud cover overlayed in their height positions and movement drifts. Therefore, usually their G_v courses are close to D_v levels and so are also ratios G_v / E_v and D_v / E_v typical for s*ituation 2*.

To document cloudy half-days were chosen from the Bratislava data again seasonally typical cases, i.e. a summer day 3rd June 2007, an autumn day on 5th September 2007, a cloudy winter morning on 20th December 2006 and a spring morning on 5th April 2006. The measured half-day courses of global horizontal illuminance G_v and diffuse sky illuminance D_v are recorded in local clock time again in Fig. 10. In early morning hours under cloudy conditions G_v / E_v and D_v / E_v are almost the same as is not so noticeable from the winter course of illuminances, but evident in Fig. 11 in 1-minute or in Fig. 12 in the hourly alternative compared with Fig. 13 and 14. In this cloudy case the G_v / E_v and D_v / E_v values is very high reaching 0.25 to 0.6 level indicating a very bright but sunless winter half-day which is indicated also by the T_v lower values compared with all other cloudy samples (in Fig. 15 and 16) as well as in rather horizontal range of L_{vz} / D_v parameters in Fig. 17 and especially their averages in Fig. 18 with the data spread within the values 0.2 to 0.38 close to overcast sky (Darula & Kittler, 2004b).

Due to cloudiness overlays and turbidity changes rather high values of T_v factors have to be expected usually dependent on the solar altitude as shown in Fig. 15 or 16. However, within the half-day courses momentary unstable P_v can occur, thus there are cases also with higher average relative sunshine durations during the half-day in the range 0.1 to 0.5, but seldom over 0.5 with lower sunlight intensities, which are usually indicated by smaller peaks within the half-day course. These drab sunlight influences are documented by the small differences between G_v / E_v and D_v / E_v values when comparing Fig. 12 and 14 respectively.

Situation 3: Overcast half-days are absolutely without any sunlight and are caused by either dense layers of Stratus or Altostratus cloudiness or inversion fog when the sun position is uncertain as it cannot be seen or guessed behind the overall dense clouds. Under such conditions $G_v = D_v$, $P_v = 0$ and average relative sunshine duration during the half-day $s \leq 0.03$. While the D_v illuminance levels and the ratio D_v / E_v are quite low, usually in the range 0.02 - 0.25, the ratios L_{vz} / D_v are over 0.3 and stable during the half-day, i.e. without any dependence on the solar altitude (Darula & Kittler, 2004c). Under overcast sky conditions when sunbeam influences are absent the sky luminance patterns in all azimuth directions are uniform, so only gradation luminance distribution can cause the D_v illuminance rise from sunrise to noon.

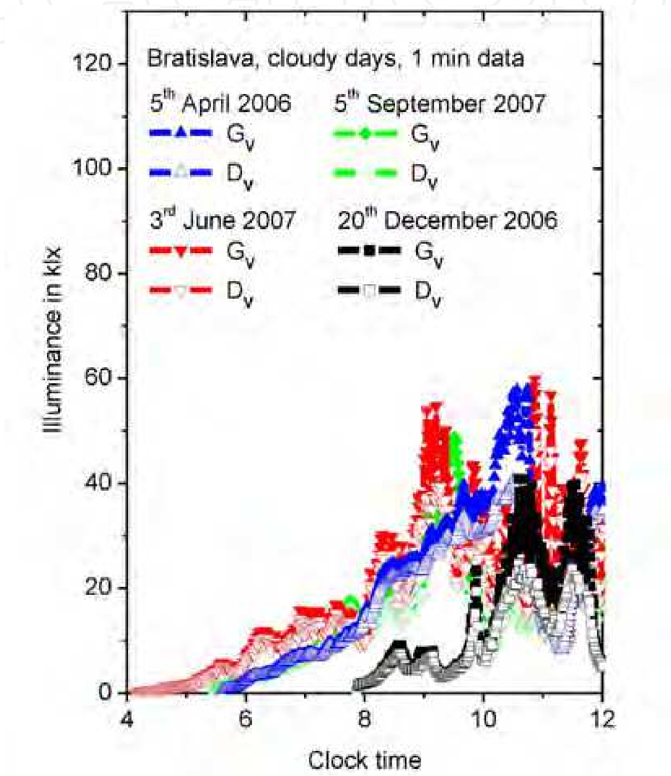

Fig. 10. Illuminance courses during cloudy morning *situations 2*

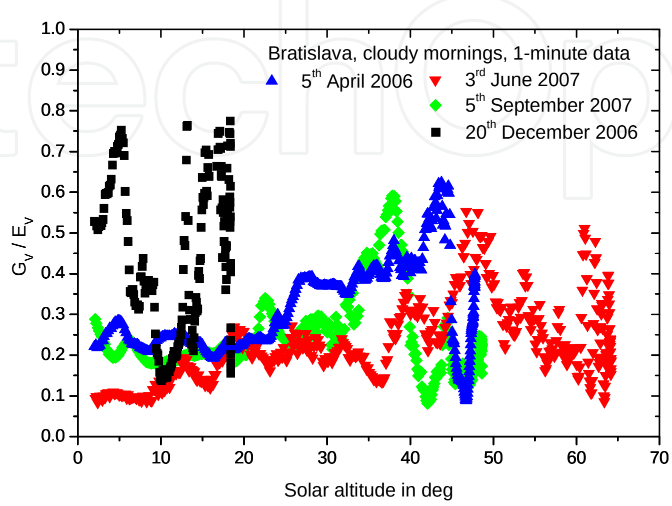

Fig. 11. G_v / E_v courses under *situation 2*: after 1-minute measurements

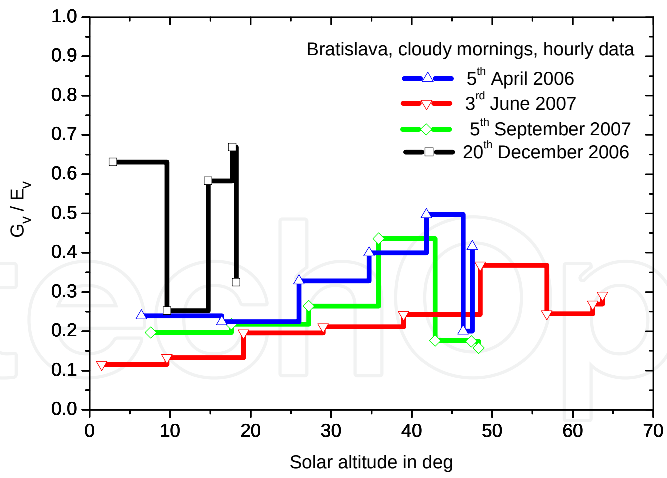

Fig. 12. G_v / E_v courses under *situation 2*: after measured hourly averages

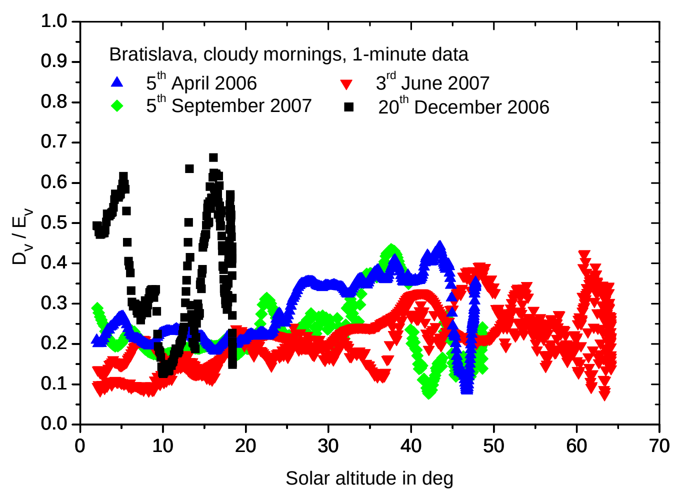

Fig. 13. D_v / E_v courses under *situation 2*: after 1-minute measurements

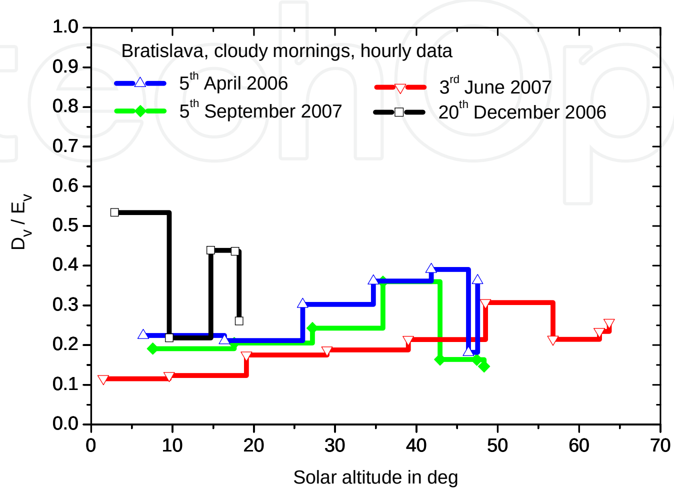

Fig. 14. D_v / E_v courses under *situation 2*: after measured hourly averages

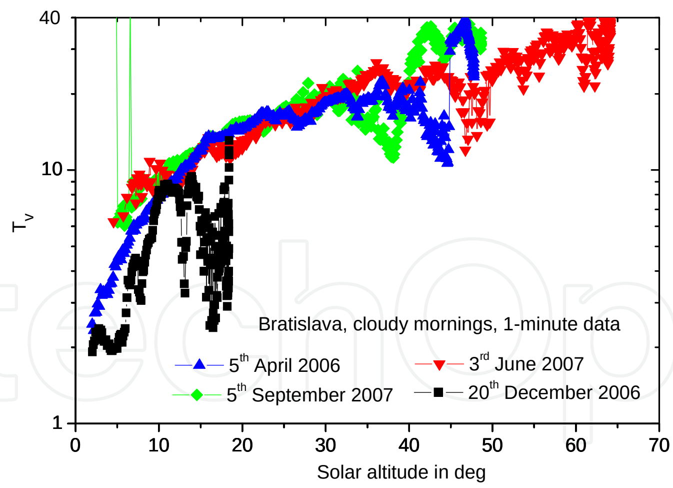

Fig. 15. T_v courses under *situation 2*: after 1-minute measurements

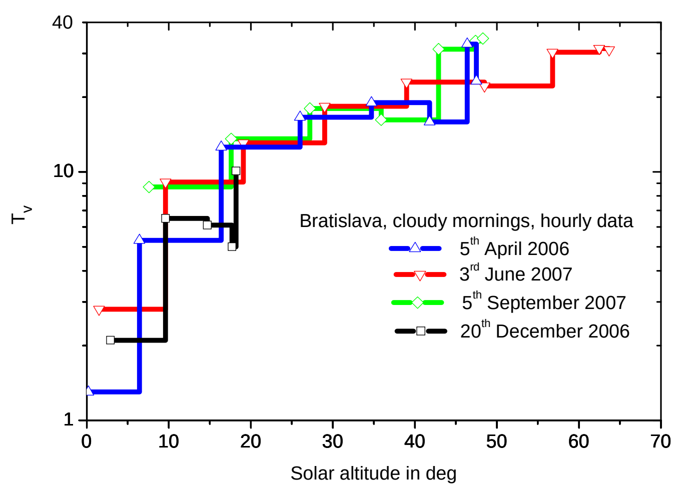

Fig. 16. T_v courses under *situation 2*: after measured hourly averages

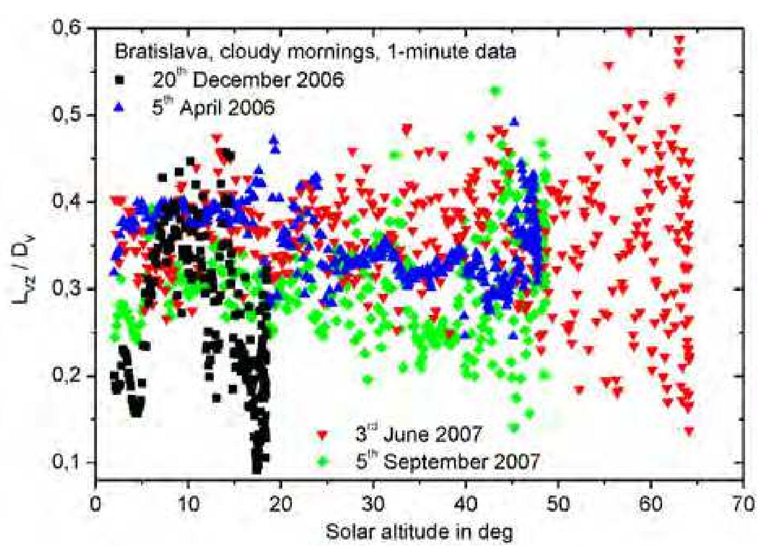

Fig. 17. L_{vz} / D_v courses under *situation 2*: after 1-minute measurements

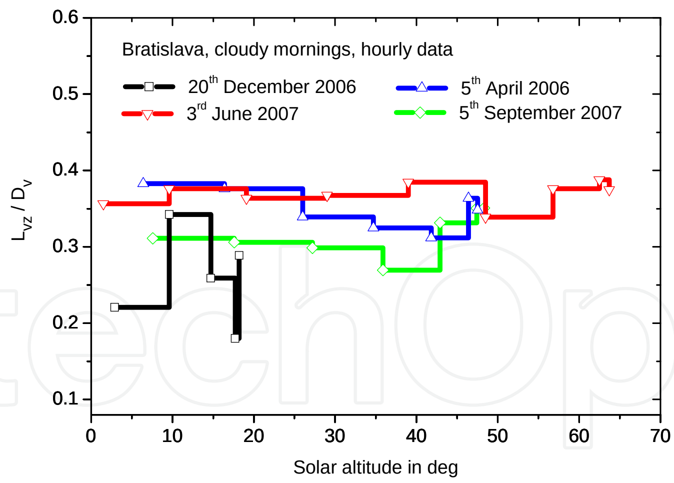

Fig. 18. L_{vz} / D_v courses under *situation* 2:after measured hourly averages

To document overcast half-days by Bratislava recordings again four seasonal examples were chosen, i.e. a winter morning on the 23rd January 2001 and a spring case on 3rd March 2001, an exceptional summer half day on 4th June 2001 and an autumn case on 6th September 2007. The half-day courses of measured global and diffuse illuminances in 1-minute intervals are in Fig. 19 with the $G_v / E_v = D_v / E_v$ analysis in Fig. 20 in 1-minute and in Fig. 21 in hourly alternatives. All four cases document the low and stable efficiency of penetration in the range 0.05-0.2 without any dependence on the solar altitude. The same stable and independent trend shows also the L_{vz} / D_v courses in Fig. 22 and 23 within the average range 0.3-0.4.

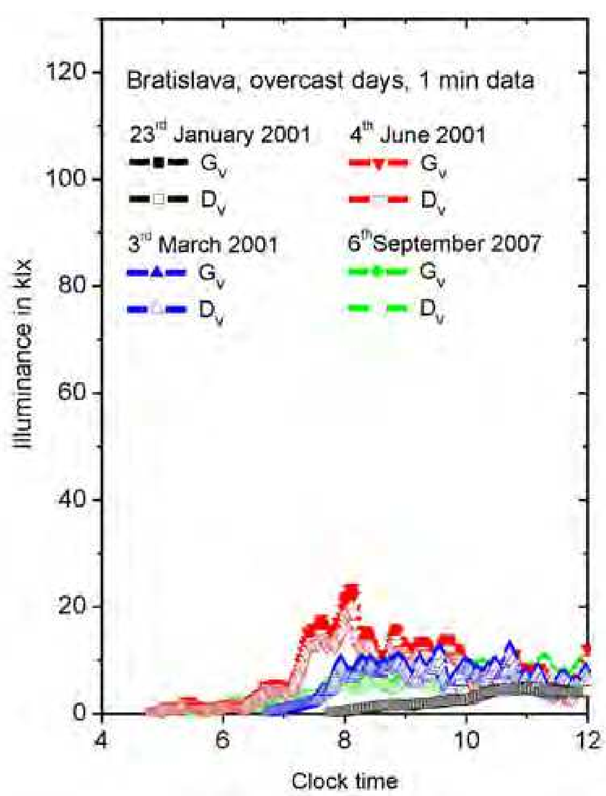

Fig. 19. Illuminance courses during overcast morning *situations 3*

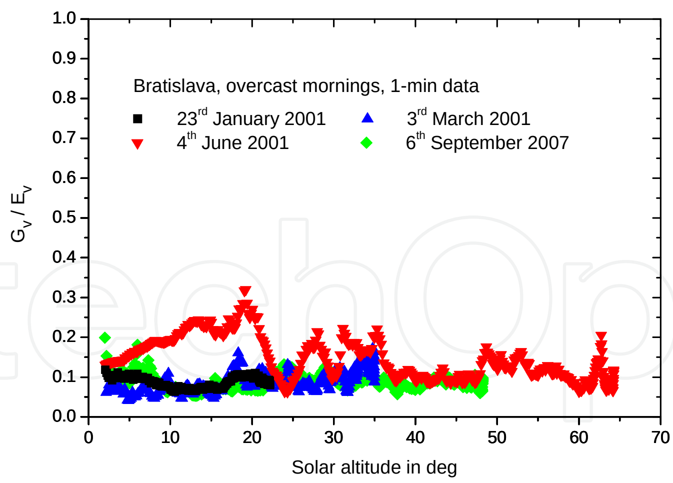

Fig. 20. G_v / E_v courses under *situation 3*: after 1-minute measurements

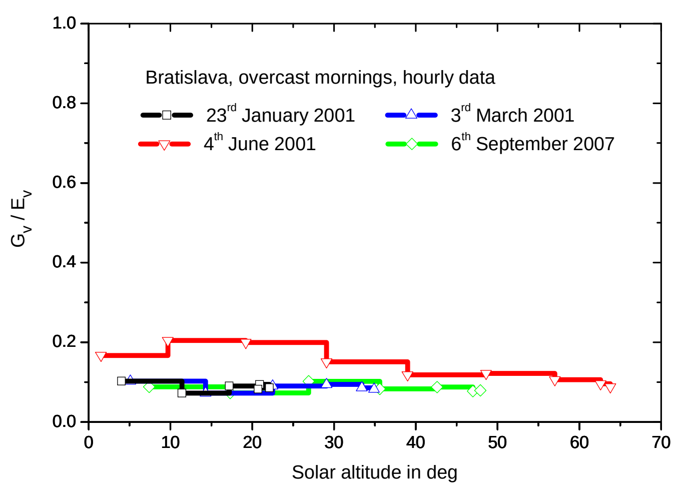

Fig. 21. G_v / E_v courses under *situation 3*:after measured hourly averages

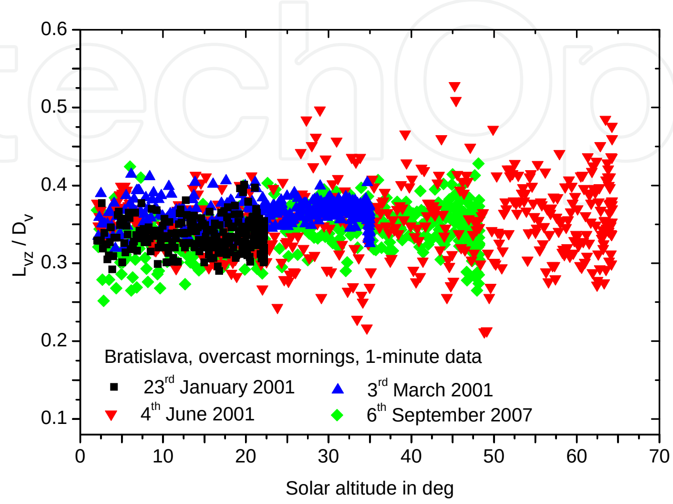

Fig. 22. L_{vz} / D_v courses under *situation 3*: after 1-minute measurements

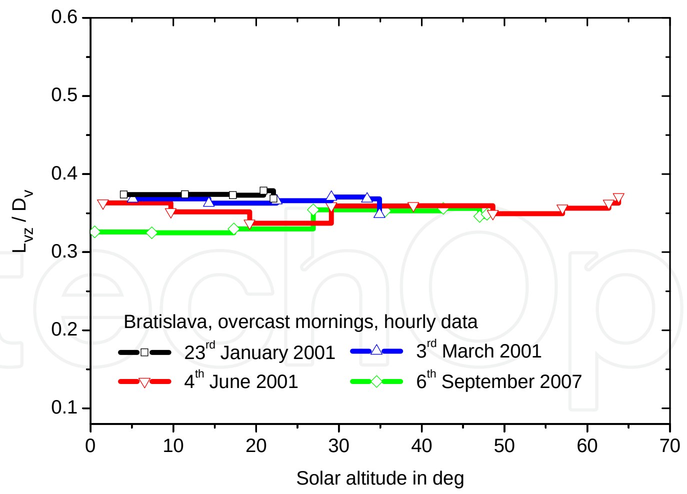

Fig. 23. L_{vz} / D_v courses under *situation 3*: after measured hourly averages

Situation 4: The dynamic courses in horizontal illuminance levels happen during those half-days when the clear sky is covered by smaller cloud patches passing the sun position and shade direct sunlight in many short-term intervals or moments. Thus the overall G_v course trends can be usually kept but with many drops of temporary loss or reduction of P_v components, which mean dynamic variations between G_v and D_v levels. Because D_v levels are not affected by the P_v changes, L_{vz} / D_v ratios indicate the sky patterns when the zenith luminance is not influenced by passing clouds significantly. However, dynamic changes are reproduced also in G_v / E_v and P_v / E_v courses. In case of dynamic situations it is problematic to use hourly averages which are levelling the momentarily occurring peaks and drops replacing them by an even horizontal line. Thus is also distorted the wide range of T_v values that have to be expected in s*ituation 4.*

Due to the irregularity and occasional movement of the shading cloud patches there is a multiple number of different cases, so the selection of characteristic courses is very problematic. However, from Bratislava data were selected also four seasonal representatives, i.e. for winter the morning on 12th January 2007, for spring 14th March 2001, for the summer example the course on 29th June 2007 and for the autumn example was chosen the dynamic morning on 26th November 2007. The actual global and diffuse illuminance courses in Fig. 24 document the dynamic changes during the chosen half-days. The same dynamic variations of G_v / E_v parameters in minute representation are in Fig. 25 while hourly means erase the highest peaks and drops (Fig. 26) considerably. The D_v / E_v courses are relatively more stable and document the low borderline (Fig. 27 and 28) from which additional sunlight influences the peaks. Similarly to G_v/E_v also L_{vz}/D_v courses are very distorted in hourly averages in Fig. 30 in comparison to 1-minute fluctuating values in Fig. 29, but the former indicate a tendency of the background spring and summer clear skies. However, these background scene is also influenced by gradually increasing turbidity, which is low with lower solar altitude and considerably rising when the sunheight is over 35 degrees (Fig. 31 and 32).

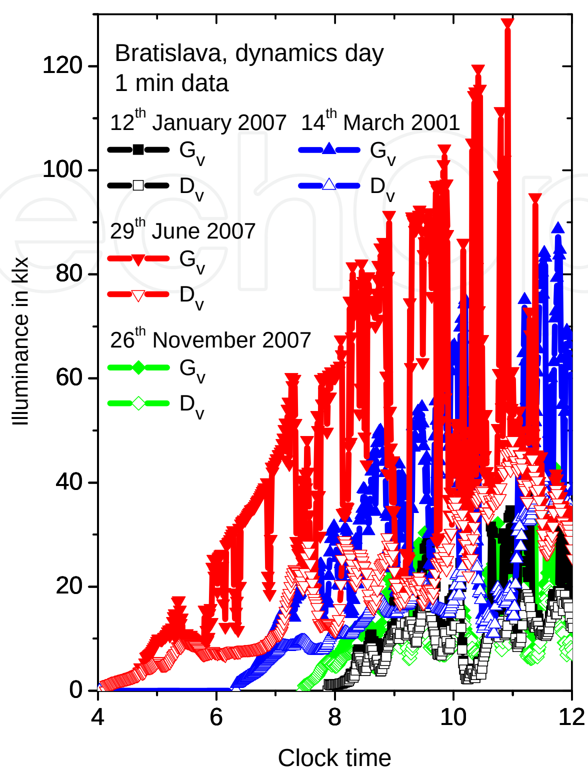

Fig. 24. Illuminance courses during overcast morning *situations 4*

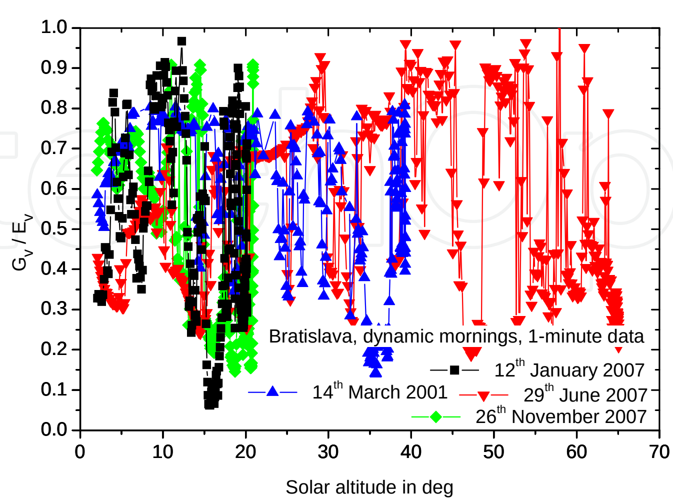

Fig. 25. G_v / E_v courses under *situation 4*: after 1-minute measurements

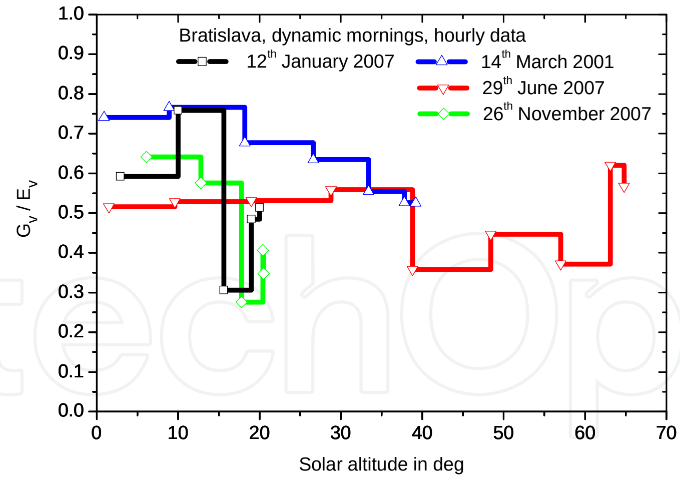

Fig. 26. G_v / E_v courses under *situation 4*: after measured hourly averages

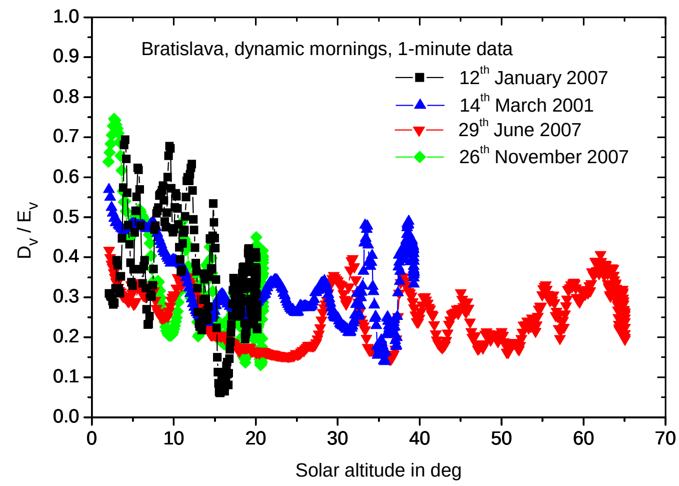

Fig. 27. D_v / E_v courses under *situation 4*: after 1-minute measurements

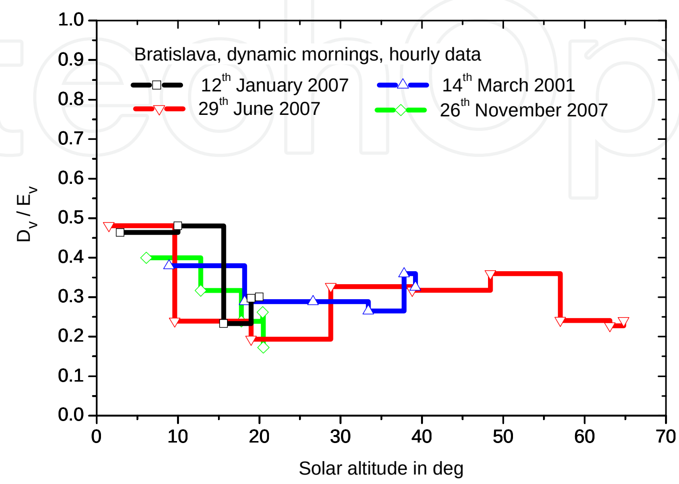

Fig. 28. D_v / E_v courses under *situation 4*:after measured hourly averages

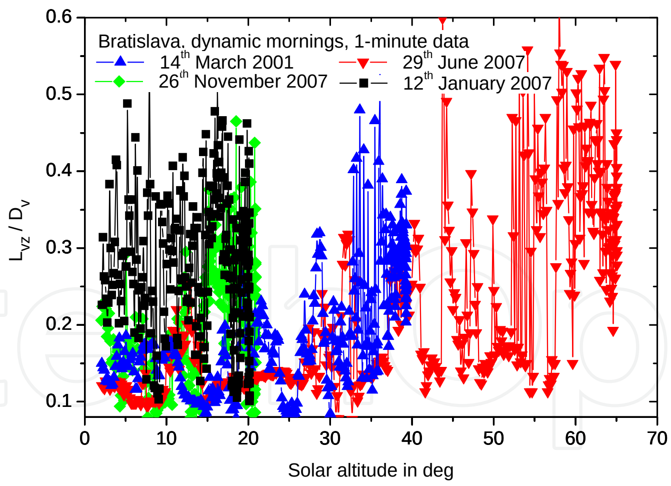

Fig. 29. $L_{vz} \,/\, D_v$ courses under *situation* 4: after 1-minute measurements

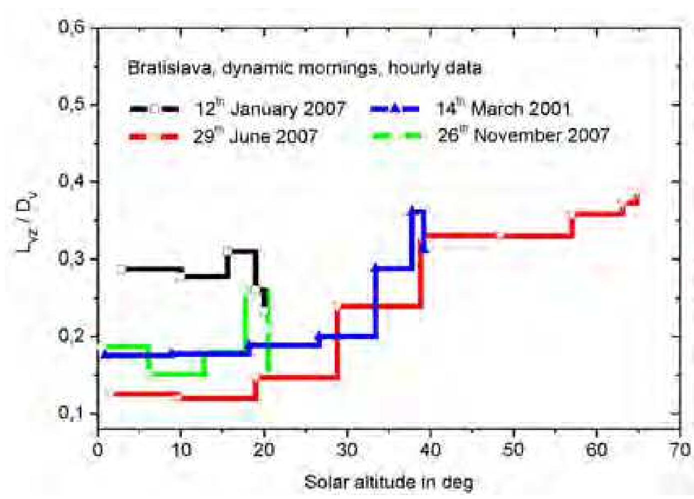

Fig. 30. $L_{vz} \,/\, D_v$ courses under *situation* 4: after measured hourly averages

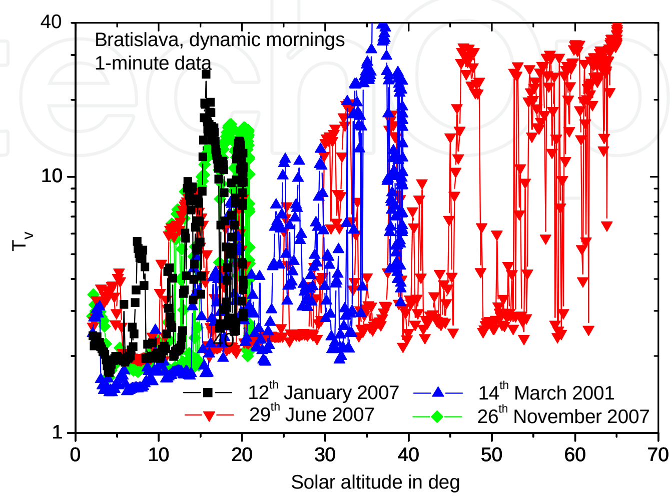

Fig. 31. T_v courses under *situation* 4: after 1-minute measurements

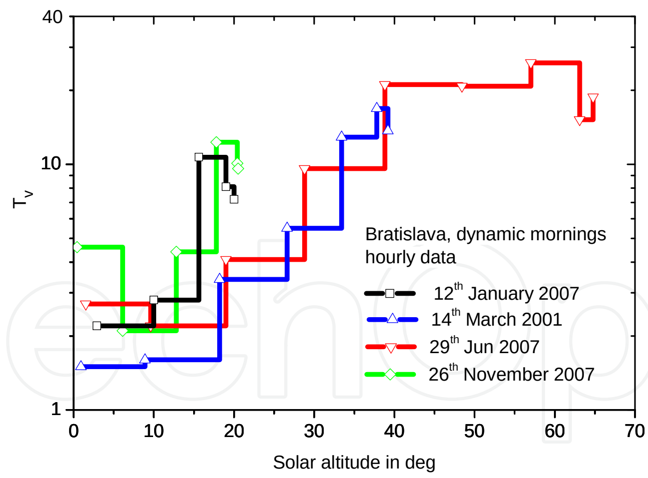

Fig. 32. T_v courses under *situation 4*:after measured hourly averages

4. Approximate dependence of the four daylight situations on relative sunshine duration

In the paper by Kittler & Darula (2002) a P-D-G diagram was published to show Bratislava 5-minute data covering the whole July 1996. From 5315 cases were 3113 with sunshine while 2202 measured cases were without sunshine according to the WMO (1983) classification. The monthly relative sunshine duration after 1-minute recordings was in July 1996 on the average $s = 0.52$ with daily changes within the range 0.022 – 0.946 which indicates the possibility of half-day situations in all four categories. Due to the averaging distortion it would seem that the prevailing sunny 5-minute intervals 3113/5315 indicate the sunshine duration roughly 0.586.

The review of daily measured illuminance courses representing July 1996 by 62 half- days can be classified into:

- *situation 1* approximately 9 morning courses and 7 in the afternoon half-day,
- *situation 2* only 2 morning courses and 2 in the afternoon half-day,
- *situation 3* only 2 morning courses and 1 in the afternoon half-day,
- *situation 4* the prevailing 18 morning and 21 afternoon half-days.

It is evident that neither the number of sunshine or sunless cases within a month in a P-D-G diagram nor L_{vz} / D_v and G_v / E_v time-averaged ratios are capable to differentiate the half-day situations when data are summarised during a day, a week or month in these mixed groups. Therefore the first step to identify, select or classify the half-day situations is to check the overall courses of G_v and D_v illuminance trends and levels and their relative efficiencies compared to the momentary extraterrestrial availability levels expressed in G_v / E_v and D_v / E_v ratios. Of course the stable or discontinuous sunshine duration follows the changes in G_v / E_v and the momentary presence of P_v / E_v ratios indicating the penetration of available extraterrestrial sunshine intensity. These half-day courses roughly characterise also the range of prevailing sky luminance patterns that can be expected and principally belong to the particular half-day situation. While situation 1 and 3 and sometimes even 2 are approximately homogeneous with evenly distributed turbidities and cloudiness cover over the whole sky vault, the situation 4 is characteristic for its unstable dynamic illuminance changes caused by complex layers of different cloud types and

distribution as well as patch movements. Thus under situation 4 can happen locally many accidental variations between quite low turbidity pockets with white-blue sky background through which direct sunshine temporarily can reach the ground while in other intervals the cloud patches cover and shade the sun beam penetration considerably.
Under homogeneous atmospheric conditions the L_{vz} / D_v ratio is quite a safe indicator of the sky luminance pattern, but during the dynamic half-day the zenith luminance as well as the sun position are influenced by passing clouds or cloud patches in several following sequence intervals.
However, for general practice and local characterisation of daylight conditions year-round long-term data are needed and should be locally available. Daylight data are also measured at the CIE IDMP stations or can be taken from the satellite database. In this respect besides global irradiation recorded in short-term variability or hourly averages at ground meteorological stations or recalculated from satellite measurements, only relative sunshine duration in daily or monthly averages have a very long tradition and are evaluated in many stations world-wide.

When inspecting monthly graphs of daily illuminance courses it becomes obvious that especially during winter and summer seasons typical weather patterns last for several days with changes either during night-time or noon. Even during perfectly clear days the symmetry around noon seems to be broken by higher turbidity in afternoon hours caused by water vapour evaporated due to rising air temperature and sunshine. Furthermore, in equatorial climate have to be expected changes in cloud cover at around noon, i.e. frequent mostly clear mornings and hours before noon but rather cloudy afternoons. During the Slovak-Greek cooperation simultaneously collected data at the CIE IDMP stations in Bratislava and Athens could serve to compare four half-day situations occurring in the temperate climate of Central Europe to those in the Mediterranean region (Darula et al., 2004). Available data was gathered during relatively long period 1994-1999.

The whole set of measured data was used to analyse the relation between sunshine duration and daily courses of illuminance. Relative sunshine duration with standard deviation SD for four typical situations were investigated in number with respect to their sequence of occurrence and results are documented in Table 1. Symbol s is relative sunshine duration calculated for the whole day while sm is for the morning period when local clock time was less than 12 o´clock and sa for the afternoon relative sunshine duration when local clock time was from 12 hours to sunset.
Except for the rapid change from overcast to clear all possible changes from morning to afternoon situations were found during the long-term of six years, i.e. 2182 days or 4364 half-days. The average relative sunshine duration corresponds perfectly with the change from the morning situation to the afternoon one respecting the tendency of the following situation change.
Although the half-day characteristics and their sequences in one or few days can form a typical year simulation, within this span any time subdivision can be utilised, i.e. Bratislava 1-minute data or Bratislava and Athens 5-minute average data can serve for analysis and comparison studies of several descriptor interrelations. However, to reach an absolute symmetry in half-days due to perfect noon time all measured momentary or average values are to be recalculated from local clock time in which these were recorded to true solar time. Of course, it has to be realised that because the daytime span between sunrise and sunset is changing during the year as well as with the local latitude the relative time of a half-day element is not constant.

Situation sequence		Number of cases	*s*		*sm*		*sa*	
Morning	Afternoon		Average	*SD*	Average	*SD*	Average	*SD*
Clear	Clear	175	0,917	0,034	0,967	0,031	0,849	0,034
Clear	Cloudy	87	0,796	0,091	0,944	0,054	0,586	0,131
Clear	Overcast	4	0,506	0,027	0,868	0,032	0,003	0,004
Clear	Dynamic	70	0,818	0,094	0,941	0,037	0,655	0,165
Cloudy	Clear	9	0,649	0,148	0,512	0,185	0,839	0,038
Cloudy	Cloudy	128	0,261	0,224	0,265	0,220	0,254	0,208
Cloudy	Overcast	201	0,049	0,074	0,082	0,080	0,000	0,001
Cloudy	Dynamic	38	0,200	0,122	0,109	0,097	0,324	0,153
Overcast	Clear	0	-	-	-	-	-	-
Overcast	Cloudy	53	0,056	0,055	0,003	0,003	0,134	0,108
Overcast	Overcast	311	0,002	0,002	0,003	0,003	0,000	0,000
Overcast	Dynamic	34	0,096	0,065	0,004	0,003	0,219	0,128
Dynamic	Clear	90	0,753	0,154	0,690	0,220	0,841	0,035
Dynamic	Cloudy	160	0,383	0,208	0,467	0,227	0,267	0,210
Dynamic	Overcast	72	0,149	0,140	0,257	0,201	0,001	0,002
Dynamic	Dynamic	750	0,504	0,219	0,536	0,252	0,462	0,205
Sum of cases		2182						

Table 1. Statistical parameters of typical courses in Bratislava, 1994 -1999

Anyhow it can be assumed that in simulation programs of a daylight reference year the half-day sequences or changes will allow to model in series of about sixty cases during a specific month either the fluent and gradual or sudden changes in weather or sky types corresponding to the probability of occurrence with its proportionality to monthly averages of relative sunshine duration. At least the mentioned four half-day daylight situations have to be foreseen for modelling the complex sun-sky coexistence with cloudiness patterns in any daylight climate, although typical cases were selected only from measurements collected in Athens and Bratislava. A research report (Darula et al., 2004) contains the detail analysis with proposals of several parameters to identify the four relevant situations from measured half-day illuminance courses and the daily average relative sunshine duration. It is evident that the stable and homogeneous *situation 1* and *situation 3* can be defined by the *s* instead of sm and sa. However, the dynamically changing illuminance courses had to be identified and classified or selected to *situation 1, situation 2* or *situation 4* by introducing an additional *U* parameter. Thus

$$situation = \begin{cases} 1 & if\ s \geq 0.75\ and\ U<7,\ \tau \\ 2 & if\ s<0.75\ and\ U<7,\ \tau \\ 3 & if\ s<0.01,\ \tau \\ 4 & if\ s \geq 0.01\ and\ U \geq 7,\ \tau \end{cases}, \tag{20}$$

where

$$U = \ln\left(\frac{1}{n-1}\sum_{i=1}|x_i - x_{i+1}|\right), \tag{21}$$

and x_i and x_{i+1} are consecutive illuminance values in the half-day course.

Using these classification parameters all four daylight types are interrelated by a fluent course of half-day average G_v / E_v and D_v / E_v dependent on the half-day sunshine duration as documented in Fig. 33 and 34 containing all 1994 morning and afternoon data recorded in Bratislava and in Athens first. In the second step a more detail separation of half-day situations dependent on half-day relative sunshine duration was made for morning 1994 data (Fig. 35) and afternoon (Fig. 36) in relation to G_v / E_v parameter repeated for also D_v / E_v and P_v / E_v with the best fit simulation of their dependence on the half-day relative sunshine duration. However, as most frequently are available only monthly relative sunshine durations in meteorological station reports the probability of occurrence of the morning and afternoon half-day situations was sought first for 1994 data (example in Fig. 37 for *situation 1*) and checked for 1991-2001 data. Thus best fit probability for the monthly redistribution simulation of morning and afternoon *situations 1* to *4* were predetermined solely dependent on the monthly relative sunshine duration using curves in Fig. 38 for morning half-days or in Fig. 39 for afternoons (Darula et al., 2004 and Darula & Kittler, 2005b).

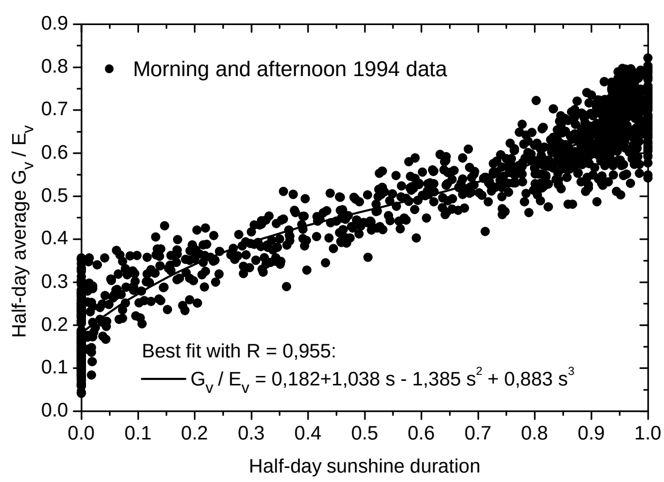

Fig. 33. Morning and afternoon G_v / E_v data after Bratislava and Athens measurements during 1994

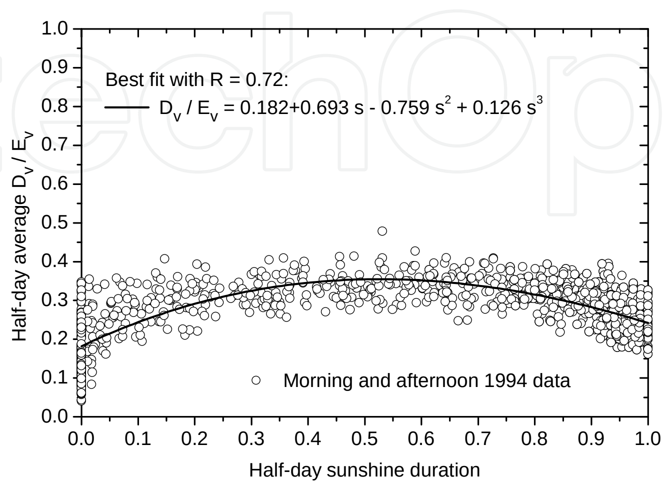

Fig. 34. Morning and afternoon D_v / E_v data after Bratislava and Athens measurements during 1994

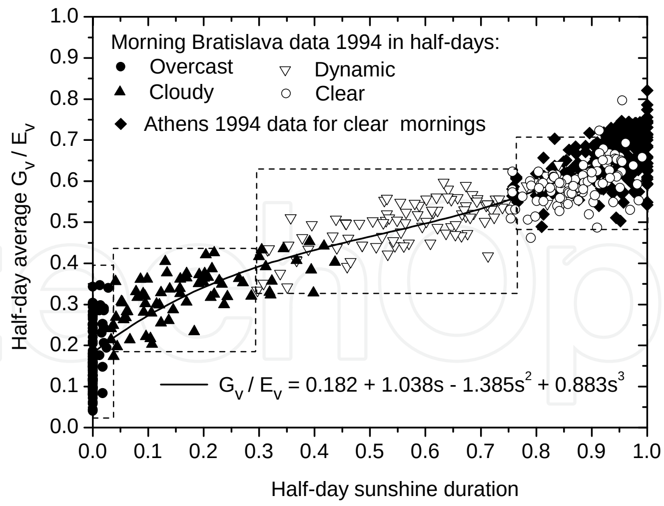

Fig. 35. Morning data for four half-day situations

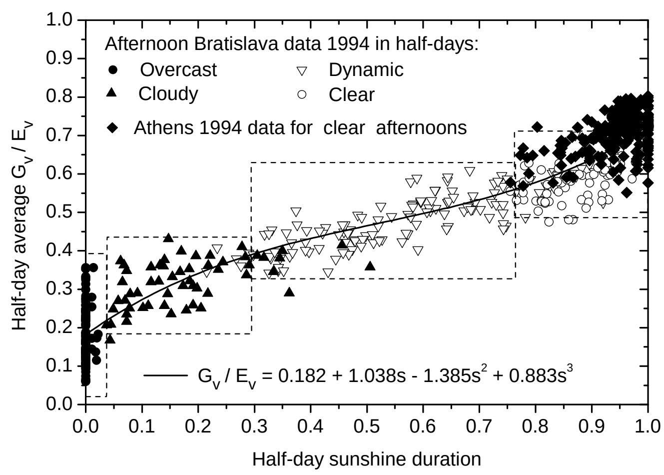

Fig. 36. Afternoon data for four half-day situations

The probability of occurrence of each of the four daylight situations in each month can be approximately estimated

- for morning half-days by:

$$Pm1 = 100\left(0.55s - 0.95s^2 + 1.65s^3\right) \ [\%], \tag{22}$$

except if $s > 0.93$, then $Pm1 = 100$

$$\text{if } s = 0 - 0.5, \text{ then } Pm2 = 100s(1.5 - 1.85s) \ [\%], \tag{23}$$

$$\text{if } s = 0.5 - 0.93, \text{ then } Pm2 = 66.86(0.93 - s) \ [\%], \tag{24}$$

$$\text{if } s > 0.93 \ \ Pm2 = 0 \ [\%], \tag{25}$$

$$Pm3 = 100(1 - s)^{2.47} \ [\%], \tag{26}$$

$$Pm4 = 100 - \left(Pm1 + Pm2 + Pm3\right) \; [\%], \tag{27}$$

- for the afternoon half-days by:

$$Pa1 = 100\left(0.62s - 0.77s^2 + 1.26s^3\right) \; [\%], \tag{28}$$

except if $s > 0.97$, then $Pa1 = 100$

$$\text{if } s = 0 - 0.5, \text{ then } Pa2 = 100s(1.2 - 1.6s) \; [\%], \tag{29}$$

$$\text{if } s = 0.5 - 0.93, \text{ then } Pa2 = 46.51(0.93 - s) \; [\%], \tag{30}$$

$$\text{if } s > 0.93 \;\; Pa2 = 0 \;\; [\%], \tag{31}$$

$$Pa3 = 100(1 - s)^{2.7} \; [\%], \tag{32}$$

$$Pa4 = 100 - \left(Pa1 + Pa2 + Pa3\right) \; [\%]. \tag{33}$$

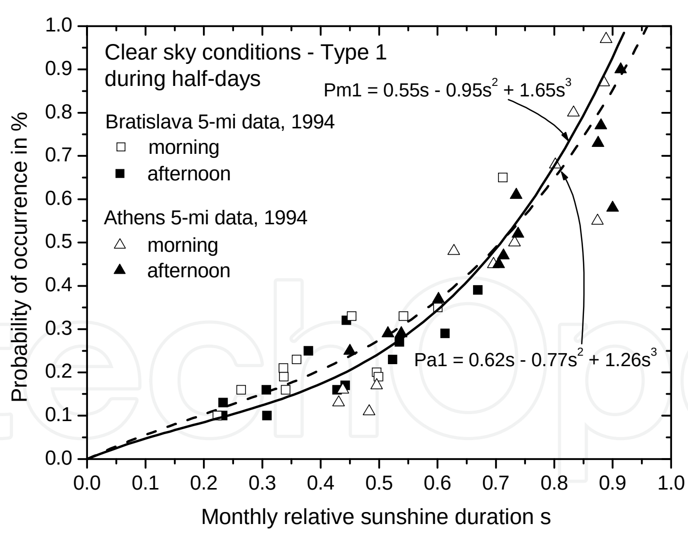

Fig. 37. Relation of clear situation to monthly relative sunshine duration in Bratislava and Athens

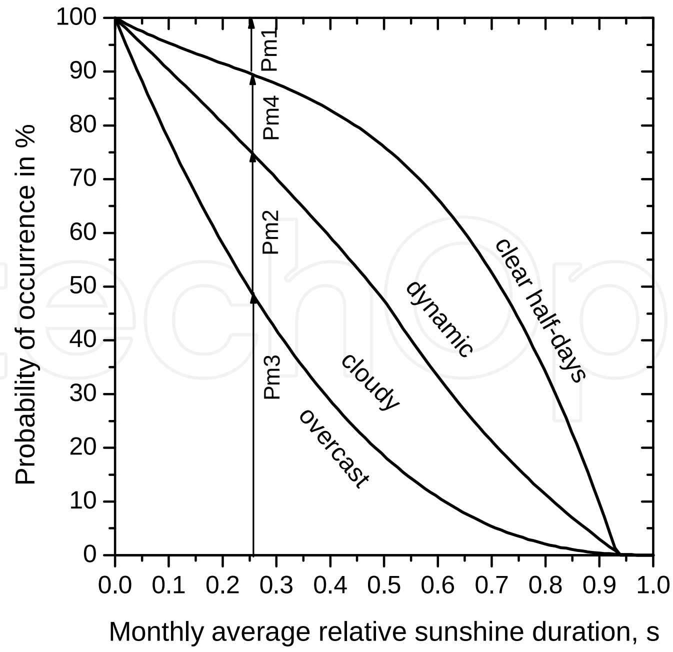

Fig. 38. Occurrence probability of half-day situations during mornings

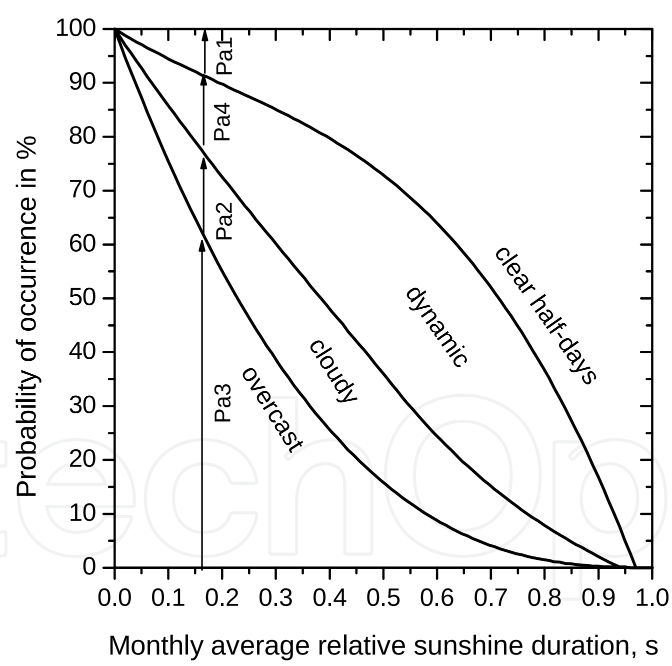

Fig. 39. Occurrence probability of half-day situations during afternoons

These probabilities of the occurrence of typical four daylight situations were derived from measurements in two different climate zones, i.e. in Bratislava as well as in Athens. So, it can be assumed that the dependence on monthly sunshine durations during morning and afternoon half-days could be valid not only in Central Europe and European Mediterranean regions but also world-wide.

5. Approximate redistribution of the four daylight situations in the yearly simulation of their occurrence

In accordance with the probability study of the four daylight situations in Bratislava morning and afternoon data during 1994-2001 the check was done using Athens data gathered in a five year period 1992-1996 (Darula et al., 2004). Because the calculated probability had to be substituted by a concrete number of days within a particular month, i.e. in integer numbers, these had to correspond with sum of half-days in that actual month. The redistribution into half-days had to dependent also on the overall monthly sunshine duration, so the redistribution model correlating the probability percentage and number of half-day situations had to be found. The best fit final solution is documented for the morning redistribution model with results shown in Fig. 40 as well as for afternoon in Fig. 41 with monthly relative sunshine duration data measured during mornings *sm* and measured during afternoons *sa*.

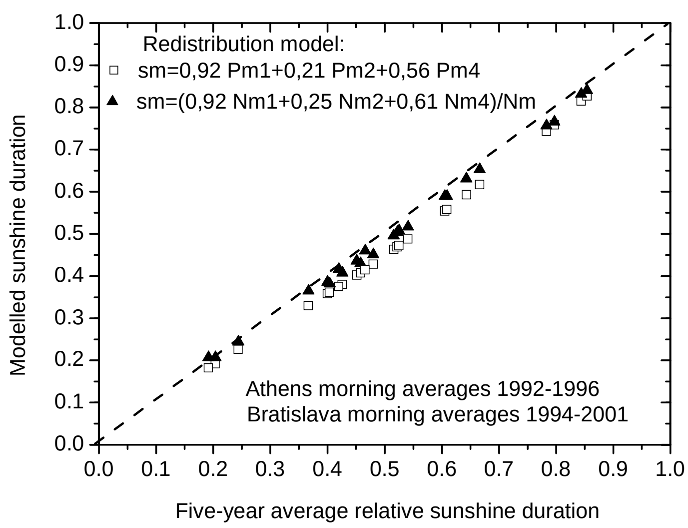

Fig. 40. Redistribution model after Bratislava and Athens morning data

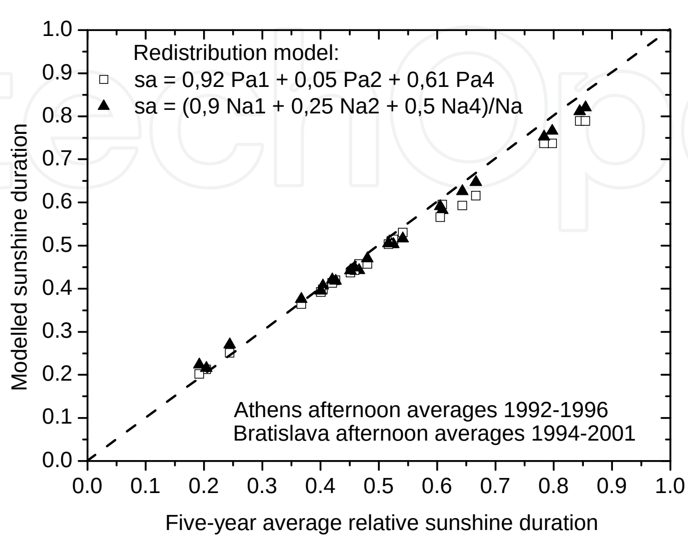

Fig. 41. Similar redistribution for afternoon half-days

In these figures besides the probability percentage notation $Pm1 - Pm4$ and $Pa1 - Pa4$ a similar notation for the number of half-days is used $Nm1 - Nm4$ and $Na1 - Na4$ while the overall number of morning half-days in a particular month is Nm for mornings and Na for afternoons in Fig. 40 and 41. These document and confirm the redistribution model that approximates the participation of the main three situations on sunlight presence and monthly sunshine duration within the particular half-day assuming that the overcast half-day is absolutely without any sunshine, thus

$$sm = \left(0.92Nm1 + 0.25Nm2 + 0.61Nm4\right) / Nm , \tag{34}$$

and

$$sa = \left(0.9Na1 + 0.25Na2 + 0.5Na4\right) / Na \cdot \tag{35}$$

This redistribution of half-day situations during mornings and afternoons was calculated for Bratislava and Athens data and as examples are shown in Table 2 and 3 only those for morning half-days. Although the verification of these redistributions for other localities is rather complicated it is evident that the ranges of mornings sm and those measured during afternoons sa can be in every month specific too. While during overcast situations the range of $s \le 0.05$ is relatively small with G_v / E_v within the spread 0.05 - 0.35 (Fig. 35 and 36), the s ranges in dynamic situations are quite large i.e. 0.3 – 0.76 while Gv/Ev spread is approximately within 0.32 – 0.61.

Thus eq. (34) and (35) characterise the redistribution of sm and sa due to four half-day situations simulating Central European and Mediterranean daylight conditions. In other climate regions (like maritime and equatorial) or during rainy (April or May) or during monsoon months more general relations might be valid as

$$sm = \left(sm1Nm1 + sm2Nm2 + sm4Nm4\right) / Nm , \tag{36}$$

and

$$sa = \left(sa1Na1 + sa2Na2 + sa4Na4\right) / Na \cdot \tag{37}$$

Therefore in the application of this redistribution it is recommended to test whether the sm and sa for appropriate situations are within their usual ranges. Approximately this is done by checking $sm4$ and $sa4$ ranges after eq. (34) and (35). During dynamic half-days both $sm4$ and $sa4$ should be in the range 0.3 to 0.75 to be related to the rise of G_v / E_v from 0.35 to 0.6 respectively.

For an example of such a check can be taken the ten-year (1995-2004) average of relative sunshine duration in Prague, which is for May $s = 0.502$. In the book by Darula et al., (2009) after percentage probabilities the number of four half-day situations was determined (on p. 64, Tab. 5.4.1) as follows:

$Nm1 = 8$, $Nm2 = 9$, $Nm3 = 6$ and $Nm4 = 8$ with the full number of morning half-days in May $Nm = 31$;

So, after eq. (34)

$$sm4 = \frac{sm\,Nm - \left(0.92Nm1 + 0.25Nm2\right)}{Nm4} = \frac{31(0.502) - \left[\left(0.92\right)8 + \left(0.25\right)9\right]}{8} = 0.744$$

Month	s	Pm1	Nm1	Pm2	Nm2	Pm3	Nm3	Pm4	Nm4	Nm	sm
1	0,204	8,67	3	22,90	7	56,92	18	11,51	3	31	0,207
2	0,404	17,59	5	30,41	9	27,85	8	24,15	6	28	0,382
3	0,367	15,55	5	30,13	9	32,32	10	22,00	7	31	0,365
4	0,466	21,70	7	29,73	9	21,23	6	27,34	8	30	0,460
5	0,541	28,08	9	26,01	8	14,61	5	31,30	9	31	0,517
6	0,522	26,29	8	27,28	8	16,15	5	30,28	9	30	0,504
7	0,525	26,57	8	27,08	8	15,90	5	30,45	10	31	0,508
8	0,609	35,53	11	21,46	7	9,83	3	33,18	10	31	0,589
9	0,426	18,95	6	30,33	9	25,38	8	25,35	7	30	0,408
10	0,420	18,57	6	30,37	9	26,04	8	25,03	8	31	0,416
11	0,244	10,16	3	25,59	8	50,11	15	14,14	4	30	0,244
12	0,192	8,23	3	21,98	7	59,06	18	10,73	3	31	0,207

Table 2. Redistribution of half-day situations according to Bratislava morning 8 – year data related to monthly average relative sunshine duration

Month	s	Pm1	Nm1	Pm2	Nm2	Pm3	Nm3	Pm4	Nm4	Nm	sm
1	0,451	20,62	6	30,02	9	22,74	7	26,62	9	31	0,436
2	0,480	22,76	6	29,38	8	19,89	6	27,98	8	28	0,451
3	0,516	25,75	8	27,68	9	16,66	5	29,91	9	31	0,496
4	0,643	39,95	12	19,19	6	7,85	2	33,00	10	30	0,631
5	0,666	43,23	13	17,65	5	6,66	2	32,45	11	31	0,653
6	0,797	67,02	20	8,89	3	1,95	1	22,14	6	30	0,766
7	0,844	77,95	24	5,75	2	1,02	0	15,29	5	31	0,832
8	0,854	80,45	25	5,08	2	0,86	0	13,60	4	31	0,841
9	0,783	64,03	19	9,83	3	2,30	1	23,85	7	30	0,757
10	0,605	35,04	11	21,73	7	10,08	3	33,15	10	31	0,589
11	0,458	21,11	6	29,89	9	22,03	7	26,96	8	30	0,430
12	0,400	17,36	5	30,40	9	28,32	9	23,92	8	31	0,386

Table 3. Redistribution of half-day situations according to Athens morning 5 – year data related to monthly average relative sunshine duration

which means that $sm4$ = 0.744 falls to the upper range 0.75, but $sm2$ = 0.25 is suspect due to probably more sunshine intervals in May. Under such conditions probably $sm4$ = 0.61 as in eq. (34) and in May $sm2$ is higher:

$$sm2 = \frac{31(0.502) - \left[(0.92)\,8 + (0.61)8\right]}{9} = 0.369\,.$$

Similarly a November check can be done using $s = 0.195$ for Prague with $Nm1 = 3$, $Nm2 = 7$, $Nm3 = 18$ and $Nm4 = 2$ with the full number of morning half-days in November $Nm = 30$ where after eq. (34) is

$$sm4 = \frac{sm\,Nm - (0.92Nm1 + 0.25Nm2)}{Nm4} = \frac{30\,(0.195) - \left[(0.92)3 + (0.25)7\right]}{2} = 0.67$$

which suites the dynamic range and is quite close to the assumed sm4 = 0.61.
In accordance with the already approximated monthly averaged values G_v / E_v in Fig. 33, 35 and 36 as well as D_v / E_v in Fig. 34 can be simulated also roughly half-day illuminance courses as

$$G_v = \frac{G_v}{E_v}\left(LSC \in \sin\gamma_s\right) \text{ [lx]}, \tag{38}$$

where

$$G_v / E_v = 0.182 + 1.038s - 1.385s^2 + 0.883s^3 \text{ [-]}, \tag{39}$$

and

$$D_v = \frac{D_v}{E_v}\left(LSC \in \sin\gamma_s\right) \text{ [lx]}, \tag{40}$$

where

$$D_v / E_v = 0.182 + 0.693s - 0.759s^2 + 0.126s^3 \text{ [-]}. \tag{41}$$

It is evident that the course distribution of illuminances is caused by the sine of the solar angle with either the momentary sine value for the moment or for the chosen time interval. This sine of the solar altitude γ_s after eq. (2) for any hour number H during daytime in TST can be used. For a short time period a straight-line interpolation can be applied when $H = (H_1 + H_2)/2$ or a value after eq. (16) is more precise.
A further possible step to specify the site and situation dependent illuminance stimulated a study that would show the relation of the four situations on typical sky patterns or ISO (2004)/CIE (2003) standard general skies if possible. Originally these standards were derived with the specification of indicatrix and gradation function in Kittler (1995) and finally recommended for standardisation in Kittler et al., (1997).
After a detail number of 5-minute measured cases in Bratislava specifying every year within the five year 1994 - 1998 span all four daylight situations were analysed with the following results:

1. under *situation 1* were present

- during mornings over 75% of clear sky types 11, 12 and 13 with the prevailing 32.55 % of sky type 12,

- during afternoons over 76 % sky types 10, 11 and 12 with the prevailing 34.48 % of sky type 12,

2. under *situation 2* were occurring

- during mornings almost 50% of cloudy sky types 2, 3 and 4 with the prevailing 18 % of sky type 3,
- during afternoons over 46 % sky types 2, 3 and 4 with the prevailing almost 17 % of sky type 3,

3. under *situation 3* were present

- during mornings almost 72% of overcast sky types 1, 2, and 3 with the prevailing almost 27 % of sky type 2,
- during afternoons over 70 % sky types 1, 2, and 3 with the prevailing almost 27 % of sky type 2,

4. under *sitation 4* were very changeable sky patterns, but the most present were

- during mornings almost 40 % sky types 11, 12 and 13 with the prevailing over 15 % of sky type 12,
- during afternoons almost 38 % sky types 11, 12 and 13 with the prevailing almost 15% of sky type 12.

This sky type prevalence (Darula & Kittler, 2008a) was in coherence considerably also with the seasonal frequency of dominant sky types found in the seasonal distribution (Kitttler et al., 2001) with prevailing overcast skies in type 2 and 3 and clear sky types 12 and 11 in Bratislava, while in Athens the highest frequency of clear polluted sky type 13 was documented, while uniform cloudy skies 5 and 6 were the most often occurring in dull seasons. Of course, the seasonal changes in occurrence frequency of clear and overcast skies is linked with relative sunshine duration and therefore with the number of half-days in any locality. However, it is interesting that in any daylight climate there exists a number of (Lambert) overcast sky type 5 with uniform luminance sky patterns, e.g. in Bratislava five year long-term these represented 12.6 % whithin cloudy *situation 2* during morning half-days and over 14 % during afternoons whithin overcast *situation 3* these were represented by morning 8.08 % and afternoon 7.74 % presence.

More and further measurements in different locations are expected to demonstrate the site-specific and short-term variability of illuminance levels (as recently was shown for irradiance by Perez et al., 2011). Due to dynamic situations it is important to evaluate short-term (momentary 1 or 5-minute regular measurements) because estimations of using hourly insolation data from satellite-based sources can be problematic and less accurate when subhourly variability is uncertain and especially if irradiance data are recalculated via luminous efficacy into illuminances (Darula & Kittler, 2008b). Therefore long-term regular measurements in absolute illuminance values are so important to have site-specific fundamental data with the possibility to derive also half-day situations. When modelling year-round situation frequencies it is also important to randomly distribute also some sequential ocurrence of specific situations (Darula & Kittler 2002) which can occur several half-days or even days after each other as is documented in Table 4 and 5. Of course, one situation can last during the whole day, i.e. the morning situation is the same in the afternoon, but quite frequent are also changes from clear to dynamic or cloudy to dynamic and vice versa especially in summer as shown in Table 4. In winter are typical lasting same situations except dynamic in two adjacent days, while in summer all consecutive days with the same situation are quite often except overcast.

Situation sequence		Winter		Summer		Spring and autumn	
Morning	Afternoon	Number of cases	%	Number of cases	%	Number of cases	%
Clear	Clear	44	10,35	55	12,20	52	11,38
Cloudy	Cloudy	82	19,29	56	12,42	81	17,72
Overcast	Overcast	55	12,94	1	0,22	11	2,41
Dynamic	Dynamic	29	6,82	56	12,42	62	13,57
Clear	Cloudy	13	3,06	20	4,44	13	2,85
Clear	Overcast	2	0,47	0	0,00	0	0,00
Clear	Dynamic	30	7,06	109	24,17	65	14,22
Cloudy	Clear	15	3,53	6	1,33	12	2,63
Cloudy	Overcast	18	4,24	2	0,44	4	0,88
Cloudy	Dynamic	55	12,94	75	16,63	70	15,32
Overcast	Clear	0	0,00	0	0,00	0	0,00
Overcast	Cloudy	28	6,59	0	0,00	3	0,66
Overcast	Dynamic	5	1,18	0	0,00	3	0,66
Dynamic	Clear	23	5,41	31	6,87	36	7,88
Dynamic	Cloudy	25	5,88	40	8,87	45	9,85
Dynamic	Overcast	1	0,24	0	0,00	0	0,00
Sum of cases		425	100	451	100	457	100

Table 4. Occurrence of daylight situations with typical sequences in one whole day

Situation sequence		Winter		Summer		Spring and autumn	
Morning	Afternoon	Number of cases	%	Number of cases	%	Number of cases	%
Clear	Clear	13	13,27	18	21,95	20	19,05
Cloudy	Cloudy	39	39,80	14	17,07	26	24,76
Overcast	Overcast	24	24,49	0	0,00	3	2,86
Dynamic	Dynamic	3	3,06	14	17,07	18	17,14
Clear	Cloudy	0	0,00	2	2,44	0	0,00
Clear	Overcast	0	0,00	0	0,00	0	0,00
Clear	Dynamic	3	3,06	13	15,85	14	13,33
Cloudy	Clear	3	3,06	0	0,00	0	0,00
Cloudy	Overcast	1	1,02	0	0,00	0	0,00
Cloudy	Dynamic	7	7,14	10	12,20	15	14,29
Overcast	Clear	0	0,00	0	0,00	0	0,00
Overcast	Cloudy	2	2,04	0	0,00	1	0,95
Overcast	Dynamic	0	0,00	0	0,00	0	0,00
Dynamic	Clear	1	1,02	3	3,66	2	1,91
Dynamic	Cloudy	2	2,04	8	9,76	6	5,71
Dynamic	Overcast	0	0,00	0	0,00	0	0,00
Sum of cases		98	100	82	100	105	100

Table 5. Repetition of four half-day situations in conscutive two days

6. Conclusions

Architectural and building science tries to gather and apply available human knowledge for the complex, aesthetic and functional creation of sophisticated habitable and healthy spaces with best environmental qualities encompassing shelter for human live, relaxation and work activities. Of course, the urban and structural objects with different interior spaces in their architectural plans and building forms have to respect natural conditions in various geographical locations, topography, local life stile and culture with trials for optimal solutions according to requirements concerning human health and prosperity, investor tendencies, investment and maintenance costs. To satisfy a complex sum of conditions, needs, codes and standards summarised by inhabitants, investors and national institutions leads to relatively simple and realistic criteria with a reasonable and experience-based background including simplified scientifically sound knowledge.

In case of utilising insolation and daylight conditions the traditional daylight science and technology is facing novel approaches and more real enhancements. In this sense are questionable also some older daylight criteria that were still recently used since the first calculation simplifications derived in the 18th Century. The Daylight Factor, Sky factor and Sky Component of the Daylight Factor used as basic criteria in various standards assume the existence of the unit uniform sky luminance after Lambert (1760). Although such Lambert uniform skies exist world-wide these do not represent typical sky luminance patterns in any site-specific conditions especially in subtropical, tropical and equatorial regions where mostly clear sky luminance distributions prevail that cause skylight illuminance conditions added frequently by sunlight.

This study tries to show and document that site-dependent daylight illuminance levels and their changes have to be expected in short-term, half-day, monthly or yearly variations in a realistic range under four typical half-daily situations. These situations can be classified with respect to relevant parameters which are dependent on extraterrestrially available illuminance reduced by atmospheric optical depth and air mass, turbidity and cloudiness conditions in site-specific variability. For practical purposes the probability of occurrence frequency of a particular half-day situation is related to the half-day or monthly relative sunshine duration which in absence of special measurements is available from many meteorological records world-wide. These monthly relative sunshine duration data can serve to estimate the local number of morning and afternoon half-day situations in any month and model their year-round expectance. Following this aim all data and figures after Bratislava and Athens CIE IDMP regular measurements can be considered as examples documenting the parameterisation and applicability of the four half-day situation system.

Current saving energy policies are also directed towards utilising renewable energy and in this respect also daylighting can serve to reduce electricity consumption in artificial illumination of interiors. A more precise determination of half-day illumination levels within year–round balance of supplementary electric lighting will enable to control it more effectively. Thus, daylight as natural source can be applied for interior illumination respecting local sunlight and skylight availability.

7. Acknowledgement

This chapter was written and partially supported under the Slovak grant project APVV-0177-10 using daylight measurements recorded by the Bratislava CIE IDMP gathered and evaluated under the Slovak VEGA grant 2/0029/11.

8. References

Bodmann, H.W. (1991). Opening of the CIE Conference by the President, *Proceedings of 22nd Session CIE*, Vol.2, p. 3

Clear, R. (1982). Calculation of turbiidity and direct sun illuminances. *Memo to Daylighting Group*. LBL, Berkeley

CIE – Commission Internationale de l´Éclairage (1994). *Guide to recommended practice of daylight measurement*. CIE Publ. 108, CB CIE, Vienna, Austria

CIE – Commission Internationale de l´Éclairage (2003). *Spatial distribution of daylight – CIE Standard General Sky*, CIE Standard S 011/E:2003, CB CIE Vienna, Austria

Cooper, P.I. (1969). The absorption of radiation in solar stills. *Solar Energy*, Vol.12, No.3, pp.333-346

Darula, S. & Kittler, R. (2002) Sekvencie situácií dennej osvetlenosti v Bratislava. (In Slovak, Sequences of daylight situations in Bratislava). *Proceedings of the 5th Intern. Conf. Light*, pp. 20-24, Brno

Darula, S. & Kittler, R. (2004a). Sunshine duration and daily courses of illuminances in Bratislava. *International Journal of Climatology*, Vol.24, No.14, pp.1777–1783

Darula, S. & Kittler, R. (2004b). New trends in daylight theory based on the new ISO/CIE Sky Standard: 2. Typology of cloudy skies and their zenith luminance. *Building Research Journal*, Vol.52, No.4, pp.245-255

Darula, S. & Kittler, R. (2004c). New trends in daylight theory based on the new ISO/CIE Sky Standard: 1. Zenith luminance on overcast skies. *Building Research Journal*, Vol.52, No.3, pp.181-197

Darula, S.; Kittler, R.; Kambezidis, H.D. & Bartzokas, A. (2004). Generation of a Daylight Reference Year for Greece and Slovakia. Final Report GR-SK 004/01. Available from ICA SAS, Bratislava.

Darula, S. & Kittler, R. (2005a). New trends in daylight theory based on the new ISO/CIE Sky Standard: 3. Zenith luminance formula verified by measurement data under cloudless skies. *Building Research Journal*, Vol.53, No.1, pp.9-31

Darula, S. & Kittler, R. (2005b). Monthly sunshine duration as a thrustworthy basis to predict annual daylight profiles. *Proceedings of the Lux Europa Session,* Berlin, pp. 141-143

Darula, S.; Kittler, R. & Gueymard, Ch. (2005). Reference luminous solar constant and solar luminance for illuminance calculations. *Solar Energy*, Vol.79, No.5, pp.559-565

Darula, S. & Kittler, R. (2008a). Occurrence of standard skies during typical daytime half-days. *Renewable Energy*, Vol.33, pp.491-500

Darula, S. & Kittler, R. (2008b). Uncertainties of luminous efficacy under various skies. *Proceedings Intern. Conf. Lighting Engineering,* Ljubljana, pp.315-322

Darula, S., Kittler, R., Kocifaj, M., Plch, J., Mohelniková, J. & Vajkaj, F. (2009). *Osvětlování světlovody*. (In Chech, Illumination by light guides). Grada Publ., Prague

Gruter, J.W. (1981). *Radiation nomenclature, definitions, symbols, units and related quantities*. Commision of the Europ. Communities, Brussels

Heindl, W. & Koch, H.A. (1976). Die Berechnung von Sonneneinstrahlungsimtensitäten für wärmetechnische Untersuchungen im Bauwesen. Gesundheits Ing., Vol. 97, No, 12, pp. 301-314

IESNA - Illuminating Engineering Society of North America (1984). Calculation Procedures Committee Recommended practice for the calculation of daylight availability. *Journal of IESNA*, Vol. 13, No. 4, pp.381-392, 1984

ISO – International Standardisation Organisation (2004). *Spatial distribution of daylight – CIE Standard General Sky,* ISO Standard 2004: 15409

Kasten, F. & Young, A.T. (1989). Revised optical air mass tables and approximation formula. *Applied Optics*, Vol.28, No.22, pp.4735-4738

Kittler, R. & Mikler, J. (1986). *Základy využívania slnečného žiarenia.* (In Slovak. Basis of the utilization of solar radiation.) Veda Publ., Bratislava

Kittler, R.; Hayman, S.; Ruck, N. & Julian, W. (1992). Daylight measurement data: Methods of evaluation and representation. *Lighting Research and Technology*, Vol.24, No.4, pp.173-187

Kittler, R. (1995). The general relationship between sky luminance patterns and exterior illuminance levels. *Proceedings of 23rd Session CIE*, Vol.1, pp.217-218

Kittler, R.; Darula, S. & Perez, R. (1997). A new generation of sky standards. *Proceedings of Lux Europa Conference*, Amsterdam, pp.359-373

Kittler, R.; Darula, S.; Kambezidis, H.D. & Bartzokas, A. (2001). Daylight climate specification based on Athens and Bratislava data. *Proceedings of the Lux Europa 2001 Conf.*, pp. 442-449, Reykjavik, Iceland

Kittler, R. & Darula, S. (2002). Parametric definition of the daylight climate. *Renewable Energy*, Vol.26, pp.177-187

Lambert, J.H. (1760). *Photometria sive de mensura et gradibus luminis, colorum et umbrae.* Augsburg, German translation by Anding, E.: *Lamberts Fotometrie*. Klett Publ., Leipzig (1892), English translation and notes by DiLaura, D.L.: *Photometry, or on the measure and gradation of light, colors and shade*. Publ.IESNA, N.Y. (2001)

Navvab, M.; Karayel, M.; Ne´eman, E. & Selkowitz, S. (1984). Analysis of atmospheric turbidity for daylight calculations. *Energy and Buildings*, Vol.6, No.3, pp.293-303

Perez, R.; Kivalov, S.; Schlemmer, J.; Hemker Jr., K. & Hoff, T. (2011) Parametrisation of site-specific short-term irradiance variability. *Solar Energy*, Vol.85, No.7, pp.1343-1353

Pierpoint, W. (1982). *Recommended practice for the calculation of daylight availability*. Draft US IES Daylight Guide

WMO – World Meteorological Organization (1983). *Guide to meteorological instruments and methods of observation*, 5th edition, No.8, pp. 9.53-9.55, World Meteorological Organization, Geneva

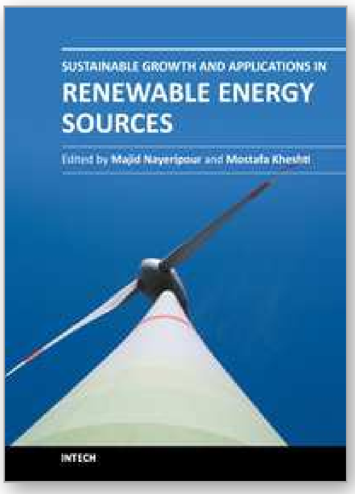

Sustainable Growth and Applications in Renewable Energy Sources

Edited by Dr. Majid Nayeripour

ISBN 978-953-307-408-5
Hard cover, 338 pages
Publisher InTech
Published online 02, December, 2011
Published in print edition December, 2011

Worldwide attention to environmental issues combined with the energy crisis force us to reduce greenhouse emissions and increase the usage of renewable energy sources as a solution to providing an efficient environment. This book addresses the current issues of sustainable growth and applications in renewable energy sources. The fifteen chapters of the book have been divided into two sections to organize the information accessible to readers. The book provides a variety of material, for instance on policies aiming at the promotion of sustainable development and implementation aspects of RES.